# An Adaptive Search Algorithm for Detecting Respiratory Artifacts Using a Wireless Passive Wearable Device

*P. O'Neill*[1], *W. M. Mongan*[1], *R. Ross*[1], *S. Acharya*[2], *A. Fontecchio*[2], *K. R. Dandekar*[2]

1. College of Computing and Informatics: Drexel University, Philadelphia, PA USA
2. College of Engineering: Drexel University, Philadelphia, PA USA
{po73, wmm24, rr625, sa427, af63, krd26}@drexel.edu

***Abstract*—With the use of a wireless, wearable, passive knitted smart fabric device as a strain gauge sensor, the proposed algorithm can estimate biomedical feedback such as respiratory activity. Variations in physical properties of Radio Frequency Identification (RFID) signals can be used to wirelessly detect physiological processes and states. However, it is typical for ambient noise artifacts to appear in the RFID signal making it difficult to identify physiological processes. This paper introduces a new technique for finding these repetitive physiological signals and identifying them into two states, *active* and *inactive*, using k-means clustering. The algorithm detects these biomedical events without the need to completely remove the noise components using a semi-unsupervised approach, and with these results, predict the next biomedical event using these classification results. This approach enables real-time noninvasive monitoring for use with actuating medical devices for therapy. Using this approach, the algorithm predicts the onset of respiratory activity in a simulated environment within approximately one second.**

***Index Terms*—Adaptive Signal Processing, Biomedical Signal Processing, Prediction Methods**

## I. Introduction

In the field of medicine, there are many different devices that can capture physiological data. The purpose of these pieces of equipment range from collecting a patient's heart rate, respiratory rate, blood pressure, or any other vital sign needed by medical professionals. Many of these devices are fastened to the patient to function [1] (*e.g.*, gel and velcro).

Placing equipment on babies or preterm infants increases the risk of injuring a patient and decreases the amount of body surface area available [2] [3]. The removal of these devices will disrupt the collection of data. A passive wireless knitted textile strain gauge sensor device called the Bellyband [4]–[6] can be used to help limit the number of sensors on a patient and deal with the issue of accidentally removing sensors.

### A. Bellyband

Fig. 1. A programmable mannequin Simbaby wearing the Bellyband about the abdomen. The Bellyband stretches and relaxes during respiratory activity, which is observed through changes in RF reflected from the knitted antenna on the Bellyband.

Figure 1 illustrates the Bellyband wrapped around an infant's diaphragm. The Bellyband is a wearable smart fabric that requires no power source to operate and has no need for any wires to be attached at any time during operation [6]. Using this device, the algorithm performs statistical signal processing to capture respiration rate, urinary contraction in pregnant women, or a patient's heart rate [7] [8].

The components that make up the Bellyband are a conductive fiber antenna and a RFID chip knitted into the Bellyband [4]. The Bellyband uses an interrogator antenna that sends out an Ultra High Frequency (UHF) signal at a bandwidth of 902-928 MHz. Once this signal reaches the Bellyband, the Bellyband's RFID chip is powered, and a return signal is reflected to the interrogator antenna. The return signal's information is then polled by a database system on a server [9] that includes the following data: Received Signal Strength Indicator (RSSI), Doppler shift, phase angle, and arrival time. This information is then analyzed on a server to infer biological meaning from the collected data, such as respiratory rate [7] [10] [11]. Figure 2 shows the physical setup of the Bellyband.

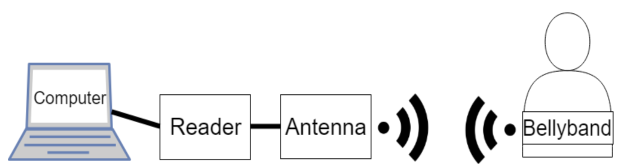


Fig. 2. The Bellyband infrastructure configuration includes an interrogator (reader) attached to an antenna which interrogates the Bellyband worn about the subject. Reflected energy from the interrogation is passively reflected back to the interrogator for processing by our algorithms running on a computer. The Bellyband contains an embedded passive MAGICSTRAP RFID LMXS31ACNA-011 chip or Monza X Dura chip, and the interrogator used is an Impinj R420 interrogator with an RFMAX S9028PCLJ antenna.

Two challenges arise when using RFID in the Bellyband. The first issue was handling noise artifacts in the return radio frequency (RF) signal from the Bellyband. There are two main causes for the noise artifacts that appear in the return signal. First, RFID technology has some inherent issues like multi-pathing, reflection, and absorption that can cause RF signals to become heavily altered or lost after being sent out from an antenna. Second, the Bellyband can be used in a hospital setting that can see a constantly changing environment. Even small changes or subject movements can have a noticeable impact causing noise artifacts to appear in the return signal. To overcome the issue of noise artifacts, the proposed algorithm uses a semi-unsupervised algorithm capable of distinguishing what is valid data from the patient [7] [10] [11].

The second issue is latency. The physical setup of the Bellyband will lead to a delay between the time a physiological event occurs (*e.g.*, breathing) and when it will be observed by the interrogator. This latency is caused by the antenna sending out an RF signal and waiting for a return RF signal from the Bellyband to reach the origin point. To compensate for this latency, our algorithm uses an unsupervised adaptive filter using the past twenty-seconds of data to predict the next physiological event. This prediction method is based on medical literature [12] [13].

### B. Paper Outline

The rest of the paper is outlined in the following Sections: related efforts are summarized in Section II; the approach for the algorithm is shown in Section III; results are shown in Section IV in which the proposed algorithm's classification capability is compared to the results from a medical device currently being used to capture respiratory activity; and finally, we conclude in Section V.

## II. Related Work

In the past twenty years, there has been considerable interest in the research and development of wearable smart fabrics that provide constant monitoring of an individual's personal health. WiBreathe is one such device [14]. Like the Bellyband, WiBreathe is capable of capturing an individual's respiration rate using RF signals. WiBreathe operates in a 2.4 GHz range that is common for most wifi devices. This gives WiBreathe the ability to track an individual's respiration rate through multiple structures (*e.g.*, walls) and removes the need to have a physical sensor on a patient. However, WiBreathe is limited because it is hard to distinguish between individuals if multiple people are in the same area. Thus, in a hospital setting, WiBreathe is not the optimal choice to capture multiple patients' respiration rates.

### A. Clustering Algorithms

The proposed algorithm clusters the data from the Bellyband into two essential states. In state 0, the patient is neither in the process of inhaling or exhaling. In state 1, the patient is in the process of respiratory activity. Due to the use of RFID technology and some of its drawbacks related to noise, these two states become confounded.

Our algorithm uses k-means clustering, and one of the issues with k-means is the need to select the number of centroids as a fixed parameter prior to processing any data. There has been research done on how to choose the number of centroids [15] with various levels of success and drawbacks. Most of the algorithms for determining the optimal amount of clusters for a particular data set attempt to break down the data into as many small clusters as possible. Although this would give us more information about our data, it would be difficult to decipher the significance of these clusters. Thus, the proposed algorithm identifies potential misclassifications made by a two centroid k-means algorithm, to avoid dividing the signal into smaller clusters. Instead, the temporal meaning of each data point and its proximity to a cluster will be resolved later in order to correct the coarse-grained classifications made into these two clusters.

### B. Respiratory Monitoring

There are many ways of recording respiration rate [16] [17]. Each of these methods have advantages and disadvantages. For instance, electrocardiograms (ECG) are capable of finding a patient's heart rate, respiration rate, and even diseases related to the patient's heart or respiration system. However, ECGs must be fastened to the patient's body in order to operate. Non-invasive ventilators (NIV) also capture a patient's respiration rate. NIVs have the advantage of allowing patients to have full body motion, while still being able to capture both the respiration rate and certain medical conditions related to the respiration system. Due to the NIV design, however, these devices are subject to some potential errors related to their use in certain environments.

The Bellyband is capable of finding a patient's heart rate, respiration rate, and certain diseases-related to a patient's respiration systems. The Bellyband offers a third option for monitoring a patient's vital signs. Instead of placing a sensor on a patient's body or in the general area around the patient, the Bellyband can be knitted into a patient's garments. This allows the patient to move freely around a room and limit the amount of sensors on the patient's body.

## III. Approach

To predict respiratory activity, preliminary processing is needed to verify that the return signal contains valid information about the patient. These pre-processing steps include removing the effects of frequency hopping III-A1, checking for a valid return signal in Section III-A2, applying noise reduction techniques in Section III-A3, and pulling information from other parts of the Bellyband's framework in Section III-A4.

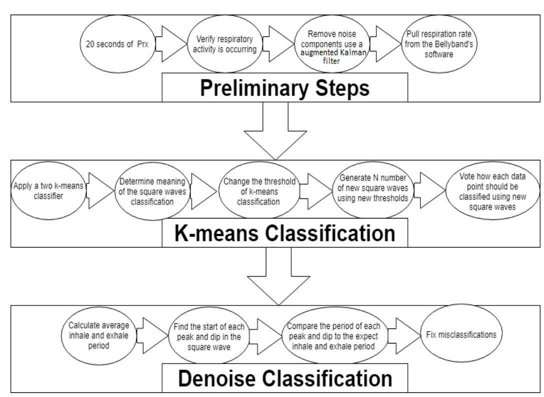


Fig. 3. High level overview of proposed algorithm

### A. Algorithm

*1) Handling Frequency Hopping:* The first step in these checks is caused by the United States Federal Communications Commission (FCC) regarding the use of single receiving antennas in the US. The FCC regulations dictate that any radio signal operating in a high-frequency range should change its frequency every 0.2 seconds, also known as frequency hopping. As a result of frequency hopping, the RSSI value from the Bellyband's return signal comes with a certain level of uncertainty. The algorithm's calculations use a modification of RSSI, which is called $P_{rx}$ defined in Equation 1 [18] [7].

$$P_{Rx,reader} = P_{Tx,reader} \times G^2_{reader} \times G^2_{tag} \left(\frac{\lambda}{4\pi r}\right)^4 \times R \quad (1)$$

where $G$ represents the gain of the tag or antenna, $P$ denotes the power, $r$ the distance between interrogator and tag, and $R$ the return path loss.

A statistical analysis using the Fisher Linear Discriminant Ratio (FDR) was performed on different RSSI features to determine optional parameters for classification [11]. The results showed a mixture of RSSI characteristics would be needed for more dependable classifications, however, noise artifacts make this process difficult.

*2) Validating Return Signal:* To confirm that respiratory activity is taking place, the algorithm implements an unsupervised algorithm to filter $P_{rx}$ with a Kalman filter which then feeds the results to a Support Vector Machine (SVM) [10] [19]. This algorithm is capable of alerting symptoms of apnea, which can be defined as a period of 10 seconds of a reduction in respiratory activity by 95% [20]. Since this algorithm can detect periods of sleep apnea, any data that is collected is considered to contain valid respiratory activity as long as no alarms are triggered.

*3) Noise Reduction:* Since the Bellyband is a wearable smart fabric that utilizes RFID technology, it is expected that some unknown quantity of noise artifacts will appear in the return signal. To limit the amount of noise in the return signal, the Bellyband uses an ARIMA model to find the best possible parameters for a Kalman filter. This process was originally used with a reference tag to help identify and remove noise artifacts [21]. For this paper, the reference tag was not used in data collection, however, some of the noise reduction techniques used with the reference tag were imported for this project. Using those imported noise reduction methods, data can be distinguished as valid increases in $P_{rx}$ compared to increases in $P_{rx}$ due to noise components [21].

*4) Estimating respiratory rate:* To estimate the respiration rate of a subject wearing the Bellyband, this algorithm uses data fusion techniques involving a Gaussian Mixture Model [7]. This estimation yields a noisy average respiratory period, which informs the voting classifier in a later step, in order to resolve misclassifications during k-means clustering (see section III-C). Because this estimate of respiratory rate is computed before the algorithm, we allow a short time (5 seconds) before starting the proposed algorithm in this paper. More detailed information about the patient's respiratory pattern is collected using a different algorithm.

Patterns recognized in the estimation of respiratory activity are subject to perturbations due to wearer properties and physical properties of respiratory artifacts including depth and duration of the breath. Fourier analysis of short time windows of respiratory data are used to infer local respiratory depth. Estimates of respiratory depth and rate are used to dynamically parameterize filtering and pre-processing of RFID-based features, which, in turn, are applied to the k-means classification algorithm. This ensures that classifications are done based on physiological data and not solely based on RSSI features.

### B. Applying k-means

The first step in the classification process is to partition the data into a rolling window of twenty seconds. Using a twenty second window allows for an adequate amount of time to train the k-means model and will narrow the impacts of averaging out the data. This sliding temporal window is classified by a k-means clustering algorithm that partitions the data into two clusters, representing applying strain to the Bellyband (*i.e.*, during respiratory movement), or stationary Bellyband (*i.e.*, non-breathing). These two clusters are represented by the "non-breathing" class, and the "breathing class" (classes 0 and 1). The result of this two k-means algorithm is a square wave representing the nearest k-means centroid to each data point seen in Figure 4. As Figure 4 shows, there is considerable fluctuation in the square wave. Low-frequency elements in $P_{rx}$ rolling window represent respiratory activity. High-frequency elements represent noise components in the $P_{rx}$ rolling window.

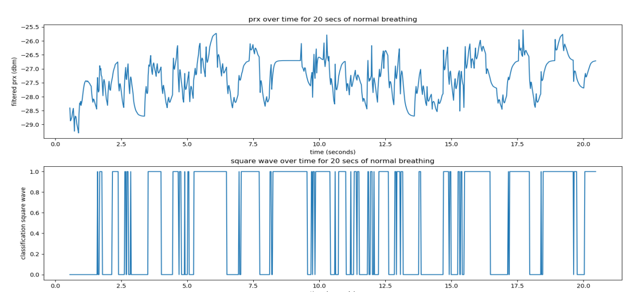


Fig. 4. k-means classification of 20 seconds of $P_{rx}$

Information from the square wave is extracted to amend errors in classification caused by noise components. To do this, we find the maximum $P_{rx}$ value and its position in the twenty second $P_{rx}$ rolling window. Then, using this location, find the corresponding value in the square wave. Whatever the value may be (0 or 1), this value will be considered what represents respiratory activity in the square wave. To understand why this is the case, consider how the Bellyband functions. As an individual inhales while wearing the Bellyband, the knitted antenna in the Bellyband stretches and is capable of returning a stronger $P_{rx}$ value due to the antenna's change in structure and subsequent change in impedance and resonant frequency. $p = argmax(P_{rx})$ in the rolling window indicates the corresponding temporal location of the peak in the square wave, and the square wave is adjusted such that this “active” cluster is always represented as state $cluster(p) = 1$.

### C. Removing noise artifacts from the square wave

In this section, possible noise artifacts are found and removed. For this approach, only data points that k-means has classified as state 0, representing the inactive will be handled.

To identify noise components, a list of acceptable percentages (LAP) are defined. LAP is a set of thresholds of the normalized distance between each data point and each of the two centroids defined by k-means. LAP can also be viewed as the accepted distance required for a data point to be classified as state 0, the inactive state. The range of percentages in LAP goes from 0% to 200%. A percent difference of 0% indicates that this data point is located exactly in the middle of the two centroids generated by k-means. Such a data point is a likely candidate for potential misclassification under k-means. If a data point is classified with a percent difference of 200%, then this data point is located exactly on one of the centroids locations. If this is the case, then there are no doubts that this data point was correctly classified by k-means. The second thing that should be noted when picking LAP percentages is that there should always be an odd number of percentages in LAP. An odd number of percentages in LAP will guarantee a tie-breaker if one should arise. In an upcoming step, multiple different square waves will be generated based on the values in LAP, and the more values that exist in LAP, the longer the time it will take to process and edit these unique square waves. In using LAP, the goal is to determine the optimal frequency that data will be marked as state 0. The method proposed will find this threshold in a semi-unsupervised way. In the final step of this approach, these thresholds are used and compared to the estimated respiration rate pulled in Section III-A4.

Next, we generate $N = |LAP|$ new square waves using the original k-means square wave, according to each threshold of the LAP. Following this, every percentage that exists in LAP is assigned to one of the N copies of the original square wave. At this point, every value in LAP has been assigned to their very own square wave that has been generated from the original k-means classifications square wave. From here, these unique percentages are assigned to each square wave and used to evaluate only the $state = 0$ data points in the square wave. To evaluate the $state = 0$ data points using LAP, we compute the percent difference for all inactive data points in the square wave using their distances from both centroids as inputs to the percent difference equation. Once these percent differences have been calculated for each data point, we compare them to the assigned percent difference to the square wave. If the results are found to be less than the assigned percent difference, then we conclude that the state of the data point is misclassified, and we update the classification to $state = 1$ (the active state).

Using the LAP square wave, we calculate the widths of all peaks (active state) and all dips (inactive state). We then apply a two k-means model to the active states to get an unsupervised way of determining what peak widths are valid in a given LAP square wave. An acceptable peak width is defined by the largest peak width identified by the two k-means models. We then update the square wave to only show accurate peak widths (see Figure 5). We repeat this process for all the generated square waves until every value that was in the LAP has been used to create a new unique square wave.

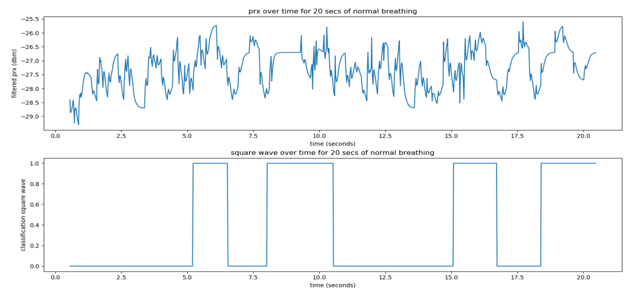


Fig. 5. k-means classification with a 175% LAP value

After these square waves have been generated, a unified denoised square wave is constructed via voting. This voting system analyzes each individual data point in the square waves. A running tally for each individual data point in the square wave determines whether or not a data point should be classified as inactive or active. The voting parameters are as follows. If a data point is classified as $state = 0$, then, this data point will cast a negative vote towards its own tally. Else, if a data point is classified as $state = 1$, then this data point will cast a positive vote towards its own tally. Once all the data points in all the square waves have been analyzed, check the running tally to see if it is either less than zero, or greater than or equal to 0 to determine the data points classification. If the tally is greater than 0, then the data point will be classified as $state = 1$. If the running tally is less than 0, then the data point will be classified as an $state = 0$. These running tallies are used to build a new square wave (see Figure 6).

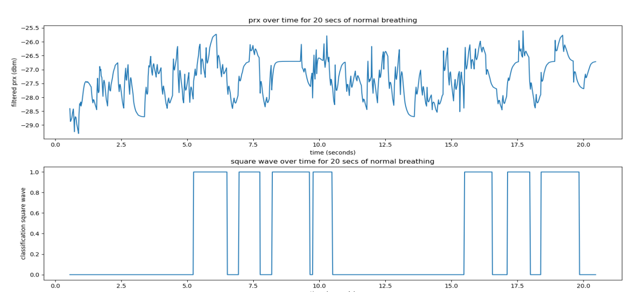


Fig. 6. Square wave after LAP vote

Using this new square wave, we classify noise components that still exist in the square wave. The first noise artifacts that will be removed are from the data points that have been marked as active. To do this, we compare the inactive data points to the active data points. We then locate the maximum $P_{rx}$ value for all the data points that are classified as inactive. Once found, we compare the $P_{rx}$ values of every point classified as active. If the max $P_{rx}$ value from the inactive data points is larger than any data point classified as active, we modify the classification from active to inactive to remove the noise artifact. The results following this step are depicted in Figure 7.

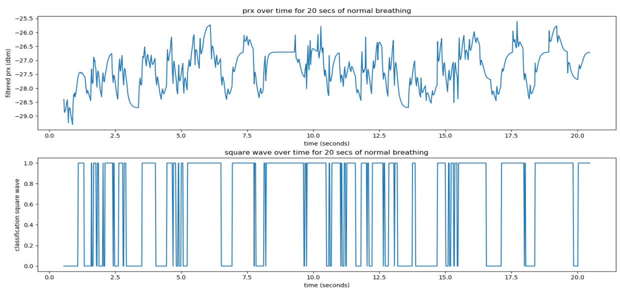


Fig. 7. Square Wave after comparing inactive and active data points

The next step in the adaptive noise reduction utility is using the respiration rate of an individual wearing the Bellyband. Using the estimated respiration rate gives an additional piece of data that indicates the expected length of each inhale and exhale. This information can then be translated to our square wave by locating the start and end times of each active and inactive period in the square wave. This can be done by looping through the square wave and identifying the times that the states change from active to inactive and vice versa. Then, we take each start and end time of each active and inactive period and subtract the start and end time to get the duration of the state. Using the duration of each state, we compare the states duration to the respiration that we pulled in section III-A4 to see the likelihood a certain period has been misclassified. If a state of active or inactive is less than the estimated time for an inhale or exhale, this state is considered to be misclassified and record its location in the rolling window.

Assuming that the square wave has at least one misclassified period, this method of noise reduction will replace some of the noise artifacts. To do this, we obtain all misclassified periods between two valid periods. Once this is found, we compute the width of both the inactive and active durations for the misclassified periods. We sum these widths and take the mean of both the active and inactive periods and compare the two to see which one is greater. Depending on the results, the entire width of the misclassified periods may be considered active or inactive, and the square wave is updated accordingly. After this step is complete, the square wave has been classified, with dynamically identified noise components removed (see Figure 8).

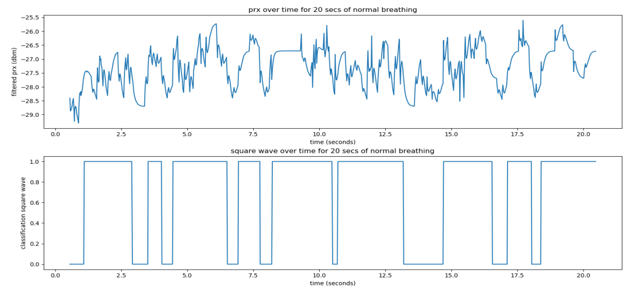


Fig. 8. Final square wave after all noise reduction and classification

| Breaths | Medical device | Bellyband |
|---|---|---|
| 1 | 1.35s | 1.08s |
| 2 | 3.36s | 3.52s |
| 3 | 5.36s | 4.44s |
| 4 | 6.92s | 6.90s |
| 5 | 8.93s | 8.23s |
| 6 | 10.94s | 10.71s |
| 7 | 12.94s | Miss |
| 8 | 14.94s | 14.70s |
| 9 | 16.82s | 17.11s |
| 10 | 18.95s | 18.39s |

TABLE I
RESULTS OF THE BELLYBAND'S CLASSIFICATION OF RESPIRATORY ACTIVITY COMPARED TO A MODERN DAY MEDICAL DEVICE CLASSIFICATION

## IV. RESULTS

The Laerdal SimBaby is a programmable mannequin that can be configured to simulate respiratory movements according to a defined rate and schedule, without external movements aside from the chest cavity motion of respiratory activity. We used the SimBaby programmable mannequin to breathe at a rate of 30 breaths per minute. The SimBaby was then hooked up to the medical device capable of capturing respiration rate. The Bellyband was then placed on the upper abdomen, and the antenna was placed roughly 30 cm away from the SimBaby.

The efficiency of our classification algorithm can best be seen when compared to a modern-day medical device that can be used in hospitals to capture respiratory activity. When doing this comparison, we place both the medical device and the Bellyband on a SimBaby to record respiratory activity. Using this method of comparison, we generate Table I that shows the Bellyband's results compare to the medical device.

Statistical analysis was performed on a minute of data captured with a SimBaby programmed to breathe at a rate of 29 breaths per minute. The null hypothesis is that the Bellyband is not comparable to the medical device used in this study, and the alternative hypothesis is that the medical device and the Bellyband are comparable. Analyzing the data using a paired-t-test with a 95% confidence interval, the results indicate that we can reject the null hypothesis (p $\approx 1 \times 10^{-5}$).

## V. CONCLUSIONS AND FUTURE WORK

Our noise classification algorithm performs well when classifying respiratory artifacts in the return signal from a device that uses the power of RFID technology, and when using those classifications to adaptively inform a prediction of upcoming respiratory behavior. To summarize our approach, we first perform preprocessing steps that involve checking to ensure that we have a valid signal, noise reductions, and pulling data from other parts of the Bellyband framework. Second, we applied k-means to a rolling window that contained $P_{rx}$ values, then, optimized k-means by using LAP. The final step is a noise reduction that involves classifying invalid structures/periods of data and classifying them to the correct state. As a result of this method, we have achieved a classification that is within an average of $\approx 0.5s$ of ground truth.

As future work, we plan to study this algorithm on human subjects. We also intend to investigate the Bellyband's structure by applying different stretchable material and testing the Bellyband on different body types, and use this algorithm to make comparisons in classification accuracy between those physical designs. Finally, we plan a formal evaluation on the relationship between respiratory artifacts and pre-processing of RFID based features using this algorithm.

## Acknowledgments

Our research results are based upon work supported by the National Science Foundation Division of Computer and Network Systems under award number CNS-1816387. Any opinions, findings, and conclusions or recommendations expressed in this material are those of the author(s) and do not necessarily reflect the views of the National Science Foundation. Research reported in this publication was supported by the National Institutes of Health under award number R01 EB029364-01. The content is solely the responsibility of the authors and does not necessarily represent the official views of the National Institutes of Health.

## References

[1] M. U. Nwankwo, J. M. Lorenz, and J. C. Gardiner, "A Standard Protocol for Blood Pressure Measurement in the Newborn," *Pediatrics*, vol. 99, no. 6, pp. e10–e10, 1997. [Online]. Available: http://pediatrics.aappublications.org/content/99/6/e10

[2] Z. Zhu, T. Liu, G. Li, T. Li, and Y. Inoue, "Wearable Sensor Systems for Infants," *Sensors*, vol. 15, pp. 3721–3749, 02 2015.

[3] H. Chen, M. Xue, Z. Mei, S. Bambang Oetomo, and W. Chen, "A Review of Wearable Sensor Systems for Monitoring Body Movements of Neonates," *Sensors*, vol. 16, no. 12, 2016. [Online]. Available: http://www.mdpi.com/1424-8220/16/12/2134

[4] W. Mongan, E. Anday, G. Dion, A. Fontecchio, K. Joyce, T. Kurzweg, Y. Liu, O. Montgomery, I. Rasheed, C. Sahin, S. Vora, and K. Dandekar, "A Multi-Disciplinary Framework for Continuous Biomedical Monitoring Using Low-Power Passive RFID-Based Wireless Wearable Sensors," in *2016 IEEE International Conference on Smart Computing, SMARTCOMP 2016*, 2016.

[5] Y. Liu, A. Levitt, C. Kara, C. Sahin, G. Dion, and K. R. Dandekar, "An Improved Design of Wearable Strain Sensor Based on Knitted RFID Technology," in *2016 IEEE Conference on Antenna Measurements Applications (CAMA)*, Oct 2016, pp. 1–4.

[6] D. Patron, W. Mongan, T. P. Kurzweg, A. Fontecchio, G. Dion, E. K. Anday, and K. R. Dandekar, "On the Use of Knitted Antennas and Inductively Coupled RFID Tags for Wearable Applications," *IEEE Transactions on Biomedical Circuits and Systems*, vol. 10, no. 6, pp. 1047–1057, Dec 2016.

[7] W. M. Mongan, R. Ross, I. Rasheed, Y. Liu, K. Ved, E. Anday, K. R. Dandekar, G. Dion, T. Kurzweg, and A. K. Fontecchio, "Data Fusion of Single-Tag RFID Measurements for Respiratory Rate Monitoring," in *IEEE Signal Processing in Medicine and Biology (SPMB)*, 2017, pp. 1–6.

[8] S. A. Vora, W. M. Mongan, E. K. Anday, K. R. Dandekar, G. Dion, A. K. Fontecchio, and T. P. Kurzweg, "On Implementing an Unconventional Infant Vital Signs Monitor with Passive RFID Tags," in *2017 IEEE International Conference on RFID, RFID 2017, Phoenix, AZ, USA, May 9-11, 2017*, 2017, pp. 47–53. [Online]. Available: https://doi.org/10.1109/RFID.2017.7945586

[9] W. M. Mongan, I. Rasheed, K. Ved, S. Vora, K. Dandekar, G. Dion, T. Kurzweg, and A. Fontecchio, "On the Use of Radio Frequency Identification for Continuous Biomedical Monitoring," in *Proceedings of the Second International Conference on Internet-of-Things Design and Implementation*, ser. IoTDI '17. New York, NY, USA: ACM, 2017, pp. 197–202. [Online]. Available: http://doi.acm.org/10.1145/3054977.3055002

[10] W. Mongan, K. Dandekar, G. Dion, T. Kurzweg, and A. Fontecchio, "Statistical Analytics of Wearable Passive RFID-based Biomedical Textile Monitors for Real-time State Classification," in *2015 IEEE Signal Processing in Medicine and Biology Symposium (SPMB)*, Dec 2015.

[11] W. Mongan, "Predictive Analytics on Real-Time Biofeedback for Actionable Classification of Activity State," PhD dissertation, Drexel University, 2018.

[12] A. Amperayani, P. Indic, C. Travers, R. Barbieri, D. Paydarfar, and N. Ambalavanan, "An Algorithm for Risk Stratification of Preterm Infants," 09 2017.

[13] U. Frey, M. G. Silverman, A. L. Barabási, and B. Suki, "Irregularities and Power Law Distributions in the Breathing Pattern in Preterm and Term Infants." *Journal of Applied Physiology*, vol. 85 3, pp. 789–97, 1998.

[14] R. Ravichandran, E. Saba, K. Chen, M. Goel, S. Gupta, and S. N. Patel, "WiBreathe: Estimating Respiration Rate Using Wireless Signals in Natural Settings in the Home," in *2015 IEEE International Conference on Pervasive Computing and Communications (PerCom)*, March 2015, pp. 131–139.

[15] D. T. Pham, S. S. Dimov, and C. D. Nguyen, "Selection of K in K-means Clustering," *Proceedings of the Institution of Mechanical Engineers, Part C: Journal of Mechanical Engineering Science*, vol. 219, no. 1, pp. 103–119, 2005.

[16] G. B. Moody, R. G. Mark, A. Zoccola, and S. Mantero, "Derivation of Respiratory Signals from Multi-lead ECGs," *Computers in Cardiology*, vol. 12, no. 1985, pp. 113–116, 1985.

[17] J.-P. Janssens, D. Adler, P. Pasquina, and O. Contal, *Contribution of Back-Up Respiratory Rate Setting in Noninvasive Ventilation*, 12 2015, pp. 673–680.

[18] Z. Su, S. Cheung, and K. Chu, "Investigation of Radio Link Budget for UHF RFID Systems," in *2010 IEEE International Conference on RFID-Technology and Applications*, June 2010, pp. 164–169.

[19] W. M. Mongan, I. Rasheed, K. Ved, A. Levitt, E. Anday, K. Dandekar, G. Dion, T. Kurzweg, and A. Fontecchio, "Real-time Detection of Apnea via Signal Processing of Time-series Properties of RFID-based Smart Garments," in *2016 IEEE Signal Processing in Medicine and Biology Symposium (SPMB)*, Dec 2016, pp. 1–6.

[20] M. Palaniswami and R. Begg, *Computational Intelligence for Movement Sciences: Neural Networks and Other Emerging Techniques (Computational Intelligence and Its Applications Series)*. Hershey, PA, USA: IGI Global, 2006.

[21] S. Acharya, W. M. Mongan, I. Rasheed, Y. Liu, E. Anday, G. Dion, A. Fontecchio, T. Kurzweg, and K. R. Dandekar, "Ensemble Learning Approach via Kalman Filtering for a Passive Wearable Respiratory Monitor," *IEEE Journal of Biomedical and Health Informatics*, pp. 1–1, 2018.